Full-Duplex Relay-Assisted OFDM-IM

Jinxian Zhao, Shuping Dang, *Member, IEEE* and Zhongli Wang

***Abstract*—In this paper, we propose a full-duplex relay-assisted orthogonal frequency-division multiplexing (OFDM) with index modulation (OFDM-IM) system, in which a complete transmission from source to destination is forwarded by a full-duplex decode-and-forward (DF) relay. By introducing full-duplex relaying, we are able to achieve a higher end-to-end capacity, as long as the power of the residual self-interference (SI) can be mitigated to an appropriate level. To investigate the proposed system, we assume the maximum-likelihood (ML) detection is adopted at both relay and destination for decoding the received OFDM block. Then, we derive or approximate the average outage probability, block error rate (BLER) and end-to-end capacity in closed form. All analyses are verified by numerical results generated by Monte Carlo simulations and comparisons between half-duplex and full-duplex relaying schemes are also provided to show the performance superiority of the proposed system.**

***Index Terms*—OFDM with index modulation (OFDM-IM), full-duplex relaying, decode-and-forward relaying, maximum-likelihood (ML) detection, performance analysis.**

I. Introduction

SINCE the standardization of orthogonal frequency-division multiplexing (OFDM) in fourth generation (4G) networks, the research related to OFDM has experienced a long period of euphoria [1]. On the other hand, in recent years, an increasing number of wireless communication applications have been found to be not satisfied by traditional OFDM, as the requirements of data rate and reliability are explosively increased [2]. Because the standardization of OFDM is related to a huge number of stakeholders and has been mature, it would be not possible to replace it by another modulation technology in a short period of time [3]. Therefore, one way to reinforce the traditional OFDM and satisfy a wide range of new wireless communication applications requiring high date rate and reliability is to introduce the index modulation (IM) and propose the new concept termed OFDM-IM, which is capable of extending the modulation dimension from two to three, including the amplitude, phase and *index of subcarrier activation pattern* [4]. Recent research works have confirmed the performance superiority of the OFDM-IM compared to traditional OFDM in terms of error rate and capacity in a variety of scenarios [5]–[8].

This work is supported by Special Funds for Technological Innovation from Harbin Science and Technology Bureau of China (grant number: 2017RAXXJ027) and Provincial Key Scientific and Technological Research Projects of the Department of Science and Technology, Jilin Province (grant number: 20170204021GX).

J. Zhao is with the College of Electronics and Information Engineering, Heilongjiang University of Science and Technology, Harbin 150022, China (e-mail: zjxusth@gmail.com)

S. Dang was with the Department of Engineering Science, University of Oxford, Oxford OX1 3PJ, U.K. and the R&D Center, Guangxi Huanan Communication Co., Ltd., Nanning 530007, P.R. China when submitting the original and revised versions of this paper (e-mail: shuping.dang@hncom.ac.cn).

Z. Wang is with the College of Electrical and Information Engineering, Beihua University, Jilin 132013, China (e-mail: wangzhongli@beihua.edu.cn).

Another attempt to further enhance the performance of OFDM-IM is to incorporate it with cooperative communications and relay networks [9]. It has also been found that such an incorporation is able to extend the coverage and improve the power efficiency [10]–[13] and even achieve spatial diversity when relay selection is applied [14], [15]. However, when employing half-duplex relaying, one apparent drawback of introducing such a cooperative framework is that the transmission must be separated by two orthogonal phases and such a separation will lead to an end-to-end capacity reduction by the fraction of the number of hops [16]. Currently, with the advances on self-interference (SI) cancellation techniques, the solution to this dilemma by introducing full-duplex relaying becomes practical and gradually comes to researchers' view [17]–[19]. In full-duplex relaying mode, a relay is capable of transmitting and receiving at the same time. Because the transmitted signal has been known by the full-duplex relay itself, it is possible to involve a series of processing techniques (e.g. analog cancellation and digital cancellation) to alleviate its destructive effects on the reception [20]–[22]. By a series of SI cancellation techniques, it is verified that the average power of the residual SI can be mitigated to the noise level and is thereby negligible, which makes the full-duplex relaying feasible in practice [22]. It has also been shown that as long as the average power of the residual SI can be reduced to a certain level, a performance gain by introducing the full-duplex relaying can be achieved [23]–[25].

Although there are some existing works, which combine multi-carrier systems and full-duplex relaying [26]–[28], to the best of authors' knowledge, there is still a gap between OFDM-IM and full-duplex relaying. To bridge the gap, we thereby propose a full-duplex relay-assisted OFDM-IM in this paper, by which the main drawback of half-duplex relaying can be mitigated. To investigate the proposed system from various aspects and obtain comprehensive performance analysis, we derive or approximate the average outage probability, block error rate (BLER) and end-to-end capacity in closed form in this paper. All analyses are substantiated by numerical results generated by Monte Carlo simulations and comparisons between full-duplex and half-duplex relaying schemes as well as with conditional OFDM without IM are also provided to confirm the performance superiority of the proposed system.

The rest of this paper is organized as follows. In Section II, we propose the system model and specify the full-duplex relaying process. Then, in Section III, we provide performance analysis in terms of average outage probability, BLER and end-to-end capacity. Following the performance analysis, numerical results are presented to verify the analysis and compare the proposed system to the OFDM-IM system using half-duplex relaying in Section IV. Finally, we conclude the paper in Section V. Table I summarizes the key notations

TABLE I: Key notations used in this paper

Notation	Definition/explanation
B_S	Length of index bits
$\bar{B}$	Average transmission rate
$\varphi(n)$	Power of the residual self-interference on the nth subcarrier
$\bar{\varphi}$	Average residual self-interference power
$G_i(n)$	Channel power gain on the nth subcarrier in the ith hop
$h_i(n)$	Channel coefficient on the nth subcarrier in the ith hop
$\mathbf{H}_i$	Diagonal channel state matrix in the ith hop
$I(n)$	Residual self-interference on the nth subcarrier
$\mathbf{I}$	Residual self-interference matrix
$\mathcal{K}$	Set of subcarrier activation patterns
K	Number of subcarrier activation patterns
$\mathcal{M}$	Set of data symbols
M	Amplitude-phase modulation order
μ_i	Average channel power gain of the ith hop
$\mathcal{N}$	Set of subcarriers
N	Number of subcarriers
N_0	Noise power
P_t	Uniform transmit power
$\mathcal{T}(k)$	Set of active subcarriers of the kth subcarrier activation pattern
$T(k)$	Number of active subcarriers of the kth subcarrier activation pattern
$\mathbf{S}(k)$	Activation state matrix of the kth subcarrier activation pattern
$\mathbf{w}_i$	Noise matrix at the receiver of the ith hop
$w_i(n)$	Noise sample on the nth subcarrier at the receiver of the ith hop
$\mathcal{X}$	Set of OFDM transmit blocks

adopted in this paper.

II. System Model

A. Transmission, Propagation and Reception

In this paper, we consider a two-hop OFDM-IM system with one source, one full-duplex decode-and-forward (DF) relay and one destination, in which N subcarriers are in use. Here, we denote the set of subcarriers as $\mathcal{N}$. Meanwhile, a sufficiently long cyclic prefix (CP) is supposed to be inserted in the transmit OFDM block, so that the transmissions over multiple subchannels can be regarded in a subcarrier basis with independent fading and interchannel interference (ICI) becomes negligible [29]. For simplicity, we also assume that there is not direct transmission link between the source and destination and thus a successful transmission must be assisted by the full-duplex DF relay. Except for the first transmission from the source initializing the full-duplex DF relay, in which the relay keeps silent, the full-duplex DF relay normally receives the current transmitted signal from the source and simultaneously forwards the processed signal from the last time slot to the destination. Because the transmit power at the relay is much larger than that of the received signal, without proper cancellation techniques, the forwarded signal yields a considerably destructive impact on the receiving module of the relay and significantly impairs the quality of received signal. Fortunately, as the forwarded signal is known by the full-duplex DF relay itself, it is possible to apply a series of complex processing techniques to alleviate its impact on the relay reception, and reduce the average power of the residual SI to the comparable level to the received signal. For clarity, we present the system model in Fig. 1.

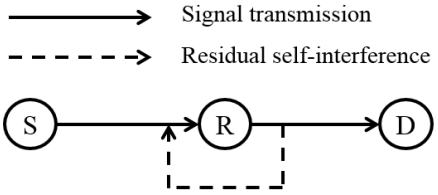

Fig. 1: Illustration of the system model considered in this paper. S: source; R: full-duplex DF relay; D: destination.

At both source and relay, the mapping relation between incoming/decoded bit streams and subcarrier activation patterns is stipulated as follows. To ease the system coordination and control, we stipulate that there exists one special subcarrier termed the *control subcarrier* and this control subcarrier is always active for continuous control signaling for network coordination and synchronization [30]. The activation states of the rest of $N-1$ subcarriers are controlled by the on-off keying (OOK) protocol according to an incoming bit stream with the length $B_S = N-1$. As a result, we can have $K = 2^{N-1}$ subcarrier activation patterns in total and we denote the set of subcarrier activation patterns as $\mathcal{K}$. Furthermore, suppose that all incoming bits are equiprobable and the number of active subcarriers denoted by $T(k) \geq 1$, $k \in \mathcal{K}$ equals to one plus the Hamming weight of the B_S-bit[1]. Assuming the multiplexing scheme is adopted in the proposed OFDM-IM system and different data symbols are conveyed on active subcarriers [31], all these data symbols are modulated by M-ary phase shift keying (M-PSK) and we denote the set of M-ary constellation symbols as $\mathcal{M}$. Here, we employ PSK, because it has been illustrated and proven that for amplitude-phase modulation (APM) in IM-based systems, the constant-envelope modulation schemes outperform the non-constant-envelope modulation schemes, e.g. quadrature amplitude modulation (QAM) [32], [33]. We can easily derive the average transmission rate in bit per channel use (bpcu) by

$$\begin{aligned}\bar{B} &= N-1+\mathbb{E}\left\{T(k)\log_2(M)\right\} \\ &= N-1+\frac{N+1}{2}\log_2(M),\end{aligned} \tag{1}$$

where $\mathbb{E}\{\cdot\}$ denotes the mean of the enclosed.

To represent a specific subcarrier activation pattern k, we can resort to the activation state matrix (ASM) of subcarriers as

$$\mathbf{S}(k) = \mathrm{diag}\{s(k,1), s(k,2), \ldots, s(k,N)\}, \tag{2}$$

where $s(k,n)$ is either '0' or '1' depending on whether the nth subcarrier is inactive or active. Note that $s(k,1) = 1$ is always true due to the utilization of the always-active control subcarrier.

[1] $T(k) \geq 1$ is because of the always-active control subcarrier and the zero-active subcarrier dilemma does not need to be considered anymore [11].

Subsequently, we can generate the transmit OFDM block by a N-point inverse fast Fourier transform (IFFT) and obtain

$$\mathbf{x}(k) = [x(m_1,1), x(m_2,2), \ldots, x(m_N,N)]^T \in \mathbb{C}^{N\times 1}, \quad (3)$$

where $(\cdot)^T$ denotes the matrix transpose operation. The entry of the transmit OFDM block $\mathbf{x}(k)$ can be written as

$$x(m_n,n) = \begin{cases} \chi_{m_n}, & n \in \mathcal{T}(k) \\ 0, & \text{otherwise} \end{cases} \quad (4)$$

where $\mathcal{T}(k)$ denotes the set of active subcarriers when the kth subcarrier activation pattern is chosen; χ_{m_n} represents a M-ary data symbol conveyed on the nth subcarrier given $m_n \in \mathcal{M}$. For simplicity, we normalize the data symbol by $\chi_{m_n}\chi^*_{m_n} = 1$.

Therefore, the information intended to be transmitted can be mapped to a unique transmit OFDM block $\mathbf{x}(k)$ and can be fully retrieved at the relay and destination by successfully estimating $\mathbf{x}(k)$.

Denote the transmit OFDM block at source and relay as $\mathbf{x}_1(k_1)$ and $\mathbf{x}_2(k_2)$. At the full-duplex DF relay, by sampling, discarding the CP, and performing the fast Fourier transform (FFT), the received OFDM block can be written as

$$\begin{aligned}\mathbf{y}_1(k_1) &= [y_1(m_1,1), y_1(m_2,2), \ldots, y_1(m_N,N)]^T \\ &= \sqrt{\frac{P_t}{T(k_1)}}\mathbf{H}_1\mathbf{x}_1(k_1) + \mathbf{S}(l)\mathbf{I} + \mathbf{w}_1 \in \mathbb{C}^{N\times 1},\end{aligned} \quad (5)$$

where $l \in \mathcal{K}$ denotes the index of the subcarrier activation pattern in the last transmission; $\mathbf{I} = [I(1), I(2), \ldots, I(N)]^T \in \mathbb{C}^{N\times 1}$ denotes the vector of N independent complex residual SI samples on each subcarrier at the relay due to the adoption of full-duplex relaying, whose entries obey $\mathcal{CN}(0,\bar{\varphi})$, and $\bar{\varphi}$ is the average residual SI power and characterizes the SI cancellation capability of full-duplex systems; $\mathbf{w}_i = [w_i(1), w_i(2), \ldots, w_i(N)]^T \in \mathbb{C}^{N\times 1}$ denotes the vector of N independent complex additive white Gaussian noise (AWGN) samples on each subcarrier in the ith hop, whose entries obey $\mathcal{CN}(0,N_0)$, and N_0 is the noise power; $\mathbf{H}_i = \text{diag}\{h_i(1), h_i(2), \ldots, h_i(N)\} \in \mathbb{C}^{N\times N}$ is a $N \times N$ diagonal channel state matrix (CSM) characterizing the channel quality in the ith hop; P_t is a uniform transmit power adopted at both source and relay.

Therefore, because of the normalization of the data symbol, the signal-to-interference-plus-noise ratio (SINR) of the received signal on the nth subcarrier (active) at the relay can be derived to be

$$\mathsf{SINR}_1(k_1,l,n) = \frac{P_t G_1(n)}{T(k_1)(s(l,n)\varphi(n) + N_0)}, \quad n \in \mathcal{T}(k_1) \quad (6)$$

where $G_i(n) = |h_i(n)|^2$ is the channel power gain and $\varphi(n) = |I(n)|^2$ denotes the power of the residual SI.

In this paper, because all subchannels regarding different subcarriers are assumed to be independent and identically distributed (i.i.d.) frequency-flat Rayleigh fading channels, the channel power gains $G_i(n)$ are i.i.d. exponentially distributed [29]. Hence, we can express the probability density function (PDF) $f_i(\zeta)$ and the cumulative distribution function (CDF) $F_i(\zeta)$ as [34]

$$f_i(\zeta) = \exp\left(-\zeta/\mu_i\right)/\mu_i \quad \Leftrightarrow \quad F_i(\zeta) = 1 - \exp\left(-\zeta/\mu_i\right), \quad (7)$$

where μ_i is the average channel power gain for the ith hop.

Meanwhile, though it is controversial [35], [36], we assume that the powers of residual SI $\varphi(n)$ obey the i.i.d. exponential distribution with mean $\bar{\varphi}$ for simplicity. As a consequence of the exponential distribution, we can write the PDF and CDF of $\varphi(n)$ as

$$f_\varphi(\zeta) = \exp\left(-\zeta/\bar{\varphi}\right)/\bar{\varphi} \quad \Leftrightarrow \quad F_\varphi(\zeta) = 1 - \exp\left(-\zeta/\bar{\varphi}\right). \quad (8)$$

The received OFDM block $\mathbf{y}_1(k)$ is decoded to yield $\mathbf{x}_2(k_2)$ to forward[2]. Similarly, at the destination, the received OFDM block is given by

$$\begin{aligned}\mathbf{y}_2(k_2) &= [y_2(m_1,1), y_2(m_2,2), \ldots, y_2(m_N,N)]^T \\ &= \sqrt{\frac{P_t}{T(k_2)}}\mathbf{H}_2\mathbf{x}_2(k_2) + \mathbf{w}_2 \in \mathbb{C}^{N\times 1},\end{aligned} \quad (9)$$

and the signal-to-noise ratio (SNR) on the nth subcarrier (active) can be expressed as

$$\mathsf{SNR}_2(k_2,n) = \frac{P_t G_2(n)}{T(k_2)N_0}, \quad n \in \mathcal{T}(k_2) \quad (10)$$

For block estimation, we adopt the maximum-likelihood (ML) detection scheme at the relay and destination. The estimated block for the ith hop can be produced by the criterion infra [38]:

$$\hat{\mathbf{x}}_i(\hat{k}_i) = \underset{\mathbf{x}(k)\in\mathcal{X}}{\arg\min} \left\| \dot{\mathbf{y}}_i(\dot{k}_i) - \sqrt{\tfrac{P_t}{T(k)}}\mathbf{H}_i\mathbf{x}(k) \right\|_F, \quad (11)$$

where $\|\cdot\|_F$ denotes the Frobenius norm of the enclosed matrix/vector; $\dot{\mathbf{y}}_i(\dot{k}_i)$ denotes the received OFDM block contaminated by noise in the ith hop; $\mathbf{x}(k)$ denotes the estimation trial; the full set of all possible $\mathbf{x}(k)$ is denoted as $\mathcal{X}$ and the cardinality $|\mathcal{X}| = M(M+1)^{N-1}$ (i.e. the size of search space for block estimation) characterizes the estimation complexity; $\hat{\mathbf{x}}_i(\hat{k}_i)$ denotes the estimated transmit OFDM block for the ith hop. To enable the ML detection, we suppose $\mathbf{H}_i$ (i.e. local channel state information (CSI)) can be perfectly estimated and has been known as the *a priori* knowledge at the relay and destination. This can be achieved by employing pilot and/or feedback signals [39]. Some advanced cognitive radio (CR)-based sensing techniques also enable the accurate CSI estimation [40].

B. Performance Evaluation Metrics

To evaluate the performance of the proposed full-duplex relay-assisted OFDM-IM system, we investigate its reliability, fidelity and throughput characterized by average outage probability, BLER and end-to-end capacity, respectively. To do so, we first mathematically formulate these three performance evaluation metrics in the following paragraphs.

[2]Ideally $\mathbf{x}_2(k_2) = \mathbf{x}_1(k_1)$ and $k_2 = k_1$, otherwise an estimation error occurs and will propagate to the next hop to have a negative impact on the estimation at the destination, which refers to the *error propagation problem* in DF relay networks [37].

1) Average outage probability: Following the definition given in [41], we define the outage event of the proposed full-duplex DF relay-assisted OFDM-IM system in an *end-to-end* manner as follows.

Definition 1: An outage event is said to occur once the received SINR or SNR regarding any of the active subcarriers at either the relay or the destination falls below a preset outage threshold s.

In accordance with *Definition 1*, the conditional end-to-end outage probability on the subcarrier activation patterns k and l can be written as[3]

$$P_o(s|k,l) = \mathbb{P}\left\{\left\{\bigcup_{n\in\mathcal{T}(k)}\{\mathsf{SINR}_1(k,l,n) < s\}\right\} \bigcup \left\{\bigcup_{n\in\mathcal{T}(k)}\{\mathsf{SNR}_2(k,n) < s\}\right\}\right\}, \tag{12}$$

where $\mathbb{P}\{\cdot\}$ denotes the probability of the event enclosed.

Furthermore, to cover all K subcarrier activation patterns, we can simply average the conditional outage probability $P_o(s|k,l)$ over subcarrier activation patterns k as well as l and thereby obtain the *average outage probability* as:

$$\bar{P}_o(s) = \mathop{\mathbb{E}}_{k,l\in\mathcal{K}}\left\{P_o(s|k,l)\right\}, \tag{13}$$

which can be used to characterize the end-to-end reliability of two-hop full-duplex DF relay-assisted OFDM-IM systems.

2) Average BLER: Likewise, we also view the block error event from an end-to-end perspective. The conditional BLER on transmit OFDM block $\dot{\mathbf{x}}_1(\dot{k}_1)$, the last subcarrier activation pattern index l and CSMs $\mathbf{H}_1$, $\mathbf{H}_2$ as well as residual SI $\mathbf{I}$ can then be written as [42]

$$P_e(\dot{\mathbf{x}}_1(\dot{k}_1)|l,\mathbf{H}_1,\mathbf{H}_2,\mathbf{I}) = \sum_{\hat{\mathbf{x}}_2(\hat{k}_2)\neq\dot{\mathbf{x}}_1(\dot{k}_1)} P_e(\dot{\mathbf{x}}_1(\dot{k}_1)\to\hat{\mathbf{x}}_2(\hat{k}_2)|l,\mathbf{H}_1,\mathbf{H}_2,\mathbf{I}), \tag{14}$$

where $P_e(\dot{\mathbf{x}}_1(\dot{k}_1)\to\hat{\mathbf{x}}_2(\hat{k}_2)|l,\mathbf{H}_1,\mathbf{H}_2,\mathbf{I})$ denotes the conditional pairwise error probability (PEP) of the block error event, in which the original transmit block $\dot{\mathbf{x}}_1(\dot{k}_1)$ at the source is erroneously estimated to $\hat{\mathbf{x}}_2(\hat{k}_2)$ at the destination, given l, $\mathbf{H}_1$, $\mathbf{H}_2$ and $\mathbf{I}$. Again, we can average the conditional BLER over transmit OFDM block $\dot{\mathbf{x}}_1(\dot{k}_1)$, the last subcarrier activation pattern index l and CSMs $\mathbf{H}_1$, $\mathbf{H}_2$ as well as residual SI $\mathbf{I}$ to have the *average BLER* by

$$\bar{P}_e = \mathop{\mathbb{E}}_{\dot{\mathbf{x}}_1(\dot{k}_1)\in\mathcal{X},l\in\mathcal{K},\mathbf{H}_1,\mathbf{H}_2,\mathbf{I}}\left\{P_e(\dot{\mathbf{x}}_1(\dot{k}_1)|l,\mathbf{H}_1,\mathbf{H}_2,\mathbf{I})\right\}, \tag{15}$$

which can be used to evaluate the end-to-end fidelity of two-hop full-duplex DF relay-assisted OFDM-IM systems.

[3]Here, we assume perfect detection at the relay node, as long as the received SINR is larger than the preset outage threshold s, such that $k_1 = k_2 = k$. It should be noted that we adopt this assumption is merely for the simplification of mathematical derivations in the following parts, which is irrelevant to the actual transmission and detection procedures. By such a simplification, insightful and closed-form approximations of relevant performance metrics can be obtained.

3) Average end-to-end capacity: Despite reliability and fidelity, throughput is also an important performance evaluation metric characterizing the efficiency of the proposed full-duplex DF relay-assisted OFDM-IM system. In this paper, we define the capacity from the perspective of an end-to-end *link* from source to destination via relay. As we specified above, we adopt the multiplexing scheme in this paper, and thereby can employ the *max-flow min-cut theorem* to derive the conditional end-to-end capacity on subcarrier activation patterns k, l and CSMs $\mathbf{H}_1$, $\mathbf{H}_2$ as well as residual SI $\mathbf{I}$ as [43]

$$C(k|l,\mathbf{H}_1,\mathbf{H}_2,\mathbf{I}) = \sum_{n\in\mathcal{T}(k)} \min\left\{\log(1+\mathsf{SINR}_1(k,l,n)), \log(1+\mathsf{SNR}_2(k,n))\right\}. \tag{16}$$

We average the conditional end-to-end capacity over subcarrier activation patterns k, l and CSMs $\mathbf{H}_1$, $\mathbf{H}_2$ as well as residual SI $\mathbf{I}$, and obtain the *average end-to-end capacity* by

$$\bar{C} = \mathop{\mathbb{E}}_{k,l\in\mathcal{K},\mathbf{H}_1,\mathbf{H}_2,\mathbf{I}}\left\{C(k|l,\mathbf{H}_1,\mathbf{H}_2,\mathbf{I})\right\}, \tag{17}$$

which can be used to evaluate the end-to-end throughput of two-hop full-duplex DF relay-assisted OFDM-IM systems.

III. Performance Analysis

A. Outage Performance Analysis

According to *Definition 1*, the end-to-end outage event in relay-assisted systems depends on the outage events in both hops and once the received signal in either the first or second is in outage, an outage is said to occur. Because the fading and thereby the outage in both hops are independent, we can decouple the end-to-end conditional outage probability defined in (12) by two per-hop conditional outage probabilities $P_{o:1}(s|k,l)$ and $P_{o:2}(s|k)$ regarding the first and second hop as

$$\begin{aligned} P_o(s|k,l) &= 1-(1-P_{o:1}(s|k,l))(1-P_{o:2}(s|k)) \\ &= P_{o:1}(s|k,l) + P_{o:2}(s|k) - P_{o:1}(s|k,l)P_{o:2}(s|k). \end{aligned} \tag{18}$$

In particular, we can explicitly express

$$P_{o:1}(s|k,l) = \mathbb{P}\left\{\bigcup_{n\in\mathcal{T}(k)}\{\mathsf{SINR}_1(k,l,n) < s\}\right\} \tag{19}$$

and

$$P_{o:2}(s|k) = \mathbb{P}\left\{\bigcup_{n\in\mathcal{T}(k)}\{\mathsf{SNR}_2(k,n) < s\}\right\}. \tag{20}$$

Furthermore, because a sufficiently long CP has been inserted in the transmit OFDM block, the transmissions over multiple subcarriers will experience independent fading and the ICI becomes negligible. As a consequence, we can decouple both per-hop conditional outage probabilities among multiple subcarriers and reduce them by

$$P_{o:1}(s|k,l) = 1 - \prod_{n\in\mathcal{T}(k)}(1-P_{o:1}(s,n|k,l)) \tag{21}$$

and

$$P_{o:2}(s|k) = 1 - \prod_{n\in\mathcal{T}(k)} (1 - P_{o:2}(s,n|k)), \tag{22}$$

where

$$\begin{aligned} P_{o:1}(s,n|k,l) &= \mathbb{P}\left\{\mathsf{SINR}_1(k,l,n) < s\right\} \\ &= \mathbb{P}\left\{\frac{P_t G_1(n)}{T(k)(s(l,n)\varphi(n)+N_0)} < s\right\} \\ &= 1 - \frac{P_t\mu_1 \exp\left(-\frac{T(k)N_0 s}{P_t\mu_1}\right)}{P_t\mu_1 + T(k)s(l,n)\bar{\varphi}s} \end{aligned} \tag{23}$$

and

$$\begin{aligned} P_{o:2}(s,n|k) &= \mathbb{P}\left\{\mathsf{SNR}_2(k,n) < s\right\} = \mathbb{P}\left\{\frac{P_t G_2(n)}{T(k)N_0} < s\right\} \\ &= 1 - \exp\left(-\frac{T(k)N_0 s}{P_t\mu_2}\right). \end{aligned} \tag{24}$$

Then, we can average $P_o(s|k,l)$ over the last subcarrier activation pattern index l by

$$\begin{aligned} P_o(s|k) &= \mathop{\mathbb{E}}_{l\in\mathcal{K}}\{P_{o:1}(s|k,l) + P_{o:2}(s|k) \\ &\qquad - P_{o:1}(s|k,l)P_{o:2}(s|k)\} \\ &= \mathop{\mathbb{E}}_{l\in\mathcal{K}}\{P_{o:1}(s|k,l)\} + P_{o:2}(s|k) \\ &\qquad - \mathop{\mathbb{E}}_{l\in\mathcal{K}}\{P_{o:1}(s|k,l)\}P_{o:2}(s|k), \end{aligned} \tag{25}$$

where $\mathop{\mathbb{E}}_{l\in\mathcal{K}}\{P_{o:1}(s|k,l)\}$ can be written as

$$\begin{aligned} &\mathop{\mathbb{E}}_{l\in\mathcal{K}}\{P_{o:1}(s|k,l)\} \\ &\overset{(a)}{=} 1 - \prod_{n\in\mathcal{T}(k)}\left(1 - \mathop{\mathbb{E}}_{s(l,n)\in\{0,1\}}\{P_{o:1}(s,n|k,l)\}\right) \end{aligned} \tag{26}$$

and (a) is valid as the activation state of each subcarrier is independent, which does not depend on other subcarriers. Since the incoming B_S-bit stream is equiprobable, we can derive

$$\begin{aligned} &\mathop{\mathbb{E}}_{s(l,n)\in\{0,1\}}\{P_{o:1}(s,n|k,l)\} \\ &= \begin{cases} 1 - \frac{P_t\mu_1\exp\left(-\frac{T(k)N_0 s}{P_t\mu_1}\right)}{P_t\mu_1 + T(k)\bar{\varphi}s}, & n = 1 \\ 1 - \frac{1}{2}\exp\left(-\frac{T(k)N_0 s}{P_t\mu_1}\right)\left(1 + \frac{P_t\mu_1}{P_t\mu_1 + T(k)\bar{\varphi}s}\right), & n \in \mathcal{T}(k)\backslash\{1\} \end{cases} \end{aligned} \tag{27}$$

Again, because the incoming B_S-bit stream is equiprobable and all subcarrier activation patterns are thereby chosen with the same probability $1/2^{N-1}$, we can easily remove the conditional dependence on subcarrier activation pattern k and obtain the average outage probability by

$$\bar{P}_o(s) = \frac{1}{2^{N-1}}\sum_{k\in\mathcal{K}} P_o(s|k). \tag{28}$$

B. Error Performance Analysis

The analysis of the error performance for two-hop cooperative communications with full-duplex relaying is rather tough and performing such an error performance analysis would result in sophisticated expressions [44], which can provide very little insight into the proposed system. To simplify the analysis in this paper and reveal the relation among error performance and key system parameters clearly, we make an assumption that in order to estimate the correct transmit OFDM block at the destination, the estimation at the full-duplex DF relay must also be correct[4]. In other words, we omit the case where an erroneously estimated and forwarded block from the first hop is then 'erroneously' estimated to the correct block at the destination. This assumption is applicable in most cases for multi-hop cooperative communications, as the probability of such a 'two negatives make a positive' case occurring is trivial. By applying this important assumption, we can decouple the estimation process from the perspective of an end-to-end link to a per-hop basis. Therefore, we have the approximation of the conditional BLER as follows:

$$\begin{aligned} &P_e(\dot{\mathbf{x}}_1(\dot{k}_1)|l,\mathbf{H}_1,\mathbf{H}_2,\mathbf{I}) \\ &\approx 1 - (1 - P_{e:1}(\dot{\mathbf{x}}_1(\dot{k}_1)|l,\mathbf{H}_1,\mathbf{I}))(1 - P_{e:2}(\dot{\mathbf{x}}_1(\dot{k}_1)|\mathbf{H}_2)) \\ &= P_{e:1}(\dot{\mathbf{x}}_1(\dot{k}_1)|l,\mathbf{H}_1,\mathbf{I}) + P_{e:2}(\dot{\mathbf{x}}_1(\dot{k}_1)|\mathbf{H}_2) \\ &\qquad - P_{e:1}(\dot{\mathbf{x}}_1(\dot{k}_1)|l,\mathbf{H}_1,\mathbf{I})P_{e:2}(\dot{\mathbf{x}}_1(\dot{k}_1)|\mathbf{H}_2), \end{aligned} \tag{29}$$

where $P_{e:1}(\dot{\mathbf{x}}_1(\dot{k}_1)|l,\mathbf{H}_1,\mathbf{I})$ and $P_{e:2}(\dot{\mathbf{x}}_1(\dot{k}_1)|\mathbf{H}_2)$ denotes the per-hop conditional BLER for the first and second hop when $\dot{\mathbf{x}}_1(\dot{k}_1)$ is transmitted. More explicitly, we can express $P_{e:1}(\dot{\mathbf{x}}_1(\dot{k}_1)|l,\mathbf{H}_1,\mathbf{I})$ and $P_{e:2}(\dot{\mathbf{x}}_1(\dot{k}_1)|\mathbf{H}_2)$ by

$$\begin{aligned} &P_{e:1}(\dot{\mathbf{x}}_1(\dot{k}_1)|l,\mathbf{H}_1,\mathbf{I}) \\ &= \sum_{\hat{\mathbf{x}}_2(\hat{k}_2)\neq\dot{\mathbf{x}}_1(\dot{k}_1)} P_{e:1}(\dot{\mathbf{x}}_1(\dot{k}_1)\to\hat{\mathbf{x}}_2(\hat{k}_2)|l,\mathbf{H}_1,\mathbf{I}) \end{aligned} \tag{30}$$

and

$$P_{e:2}(\dot{\mathbf{x}}_1(\dot{k}_1)|\mathbf{H}_2) = \sum_{\hat{\mathbf{x}}_2(\hat{k}_2)\neq\dot{\mathbf{x}}_1(\dot{k}_1)} P_{e:2}(\dot{\mathbf{x}}_1(\dot{k}_1)\to\hat{\mathbf{x}}_2(\hat{k}_2)|\mathbf{H}_2), \tag{31}$$

where $P_{e:1}(\dot{\mathbf{x}}_1(\dot{k}_1)\to\hat{\mathbf{x}}_2(\hat{k}_2)|l,\mathbf{H}_1,\mathbf{I})$ and $P_{e:2}(\dot{\mathbf{x}}_1(\dot{k}_1)\to\hat{\mathbf{x}}_2(\hat{k}_2)|\mathbf{H}_2)$ are the conditional PEP that the transmitted OFDM block $\dot{\mathbf{x}}_1(\dot{k}_1)$ has been erroneously estimated to be $\hat{\mathbf{x}}_2(\hat{k}_2)$ in the first and second hop, respectively.

With the help of the Gaussian tail function (a.k.a. the Q-function), we can write and approximate the PEP $P_{e:1}(\dot{\mathbf{x}}_1(\dot{k}_1)\to\hat{\mathbf{x}}_2(\hat{k}_2)|l,\mathbf{H}_1,\mathbf{I})$ in (32) (shown at the top of the next page), where $Q(x) = \frac{1}{\sqrt{2\pi}}\int_x^\infty \exp\left(-u^2/2\right)\mathrm{d}u$ is the Gaussian tail function; $\Theta(n) = \dot{x}_1(\dot{m}_n,n)/\sqrt{T(\dot{k}_1)} - \hat{x}_2(\hat{m}_n,n)/\sqrt{T(\hat{k}_2)}$; $\{\lambda_1,\lambda_2\} = \{1/12, 1/4\}$; $\{\epsilon_1,\epsilon_2\} = \{1/2, 2/3\}$; (a) is approximated by assuming $\left|\sqrt{P_t}h_1(n)\Theta(n)\right|^2 \gg |s(l,n)I(n)|^2$; (b) is approximated by the relation

[4]Again, this assumption adopted is only for simplifying the mathematical derivations in the following so as to achieve an insightful and closed-form approximation of the average BLER. This is irrelevant to the actual transmission and detection procedures.

$Q(x) \approx \frac{1}{12}\exp\left(-\frac{x^2}{2}\right) + \frac{1}{4}\exp\left(-\frac{2x^2}{3}\right)$ [45]; (c) is valid due to the basic property of the exponential function: $\exp(\sum_n x_n) = \prod_n \exp(x_n)$.

Likewise, we can write the PEP $P_{e:2}(\dot{\mathbf{x}}_1(\dot{k}_1) \to \hat{\mathbf{x}}_2(\hat{k}_2)|\mathbf{H}_2)$ as

$$\begin{aligned} &P_{e:2}(\dot{\mathbf{x}}_1(\dot{k}_1) \to \hat{\mathbf{x}}_2(\hat{k}_2)|\mathbf{H}_2) \\ &= Q\left(\sqrt{\frac{P_t}{N_0}\left\|\mathbf{H}_2\left(\frac{\dot{\mathbf{x}}_1(\dot{k}_1)}{\sqrt{T(\dot{k}_1)}} - \frac{\hat{\mathbf{x}}_2(\hat{k}_2)}{\sqrt{T(\hat{k}_2)}}\right)\right\|_F^2}\right) \\ &\approx \sum_{q=1}^{2}\lambda_q \prod_{n=1}^{N}\exp\left(-\frac{\epsilon_q P_t}{N_0}G_2(n)|\Theta(n)|^2\right). \end{aligned} \tag{33}$$

According to (29), we average $P_e(\dot{\mathbf{x}}_1(\dot{k}_1)|l, \mathbf{H}_1, \mathbf{H}_2, \mathbf{I})$ over $\mathbf{H}_1$ and $\mathbf{H}_2$ as

$$\begin{aligned} P_e(\dot{\mathbf{x}}_1(\dot{k}_1)|l, \mathbf{I}) &= \mathop{\mathbb{E}}_{\mathbf{H}_1,\mathbf{H}_2}\left\{P_e(\dot{\mathbf{x}}_1(\dot{k}_1)|l, \mathbf{H}_1, \mathbf{H}_2, \mathbf{I})\right\} \\ &\approx 1 - \mathop{\mathbb{E}}_{\mathbf{H}_1}\left\{1 - P_{e:1}(\dot{\mathbf{x}}_1(\dot{k}_1)|l, \mathbf{H}_1, \mathbf{I})\right\} \\ &\qquad \times \mathop{\mathbb{E}}_{\mathbf{H}_2}\left\{1 - P_{e:2}(\dot{\mathbf{x}}_1(\dot{k}_1)|\mathbf{H}_2)\right\} \\ &= P_{e:1}(\dot{\mathbf{x}}_1(\dot{k}_1)|l, \mathbf{I}) + P_{e:2}(\dot{\mathbf{x}}_1(\dot{k}_1)) \\ &\qquad - P_{e:1}(\dot{\mathbf{x}}_1(\dot{k}_1)|l, \mathbf{I})P_{e:2}(\dot{\mathbf{x}}_1(\dot{k}_1)), \end{aligned} \tag{34}$$

where

$$P_{e:1}(\dot{\mathbf{x}}_1(\dot{k}_1)|l, \mathbf{I}) = \mathop{\mathbb{E}}_{\mathbf{H}_1}\left\{P_{e:1}(\dot{\mathbf{x}}_1(\dot{k}_1)|l, \mathbf{H}_1, \mathbf{I})\right\} \tag{35}$$

and

$$P_{e:2}(\dot{\mathbf{x}}_1(\dot{k}_1)) = \mathop{\mathbb{E}}_{\mathbf{H}_2}\left\{P_{e:2}(\dot{\mathbf{x}}_1(\dot{k}_1)|\mathbf{H}_2)\right\}, \tag{36}$$

which can be approximated according to (30), (31), (32) and (33) in closed form as shown in (37) and (38) (both shown at the top of the next page), respectively. Subsequently, we can also average $P_e(\dot{\mathbf{x}}_1(\dot{k}_1)|l, \mathbf{I})$ over the last subcarrier activation pattern l to be

$$\begin{aligned} P_e(\dot{\mathbf{x}}_1(\dot{k}_1)|\mathbf{I}) &= \mathop{\mathbb{E}}_{l\in\mathcal{K}}\left\{P_e(\dot{\mathbf{x}}_1(\dot{k}_1)|l, \mathbf{I})\right\} \\ &= P_{e:1}(\dot{\mathbf{x}}_1(\dot{k}_1)|\mathbf{I}) + P_{e:2}(\dot{\mathbf{x}}_1(\dot{k}_1)) \\ &\qquad - P_{e:1}(\dot{\mathbf{x}}_1(\dot{k}_1)|\mathbf{I})P_{e:2}(\dot{\mathbf{x}}_1(\dot{k}_1)), \end{aligned} \tag{39}$$

where $P_{e:1}(\dot{\mathbf{x}}_1(\dot{k}_1)|\mathbf{I})$ can be derived in closed form as follows:

$$\begin{aligned} P_{e:1}(\dot{\mathbf{x}}_1(\dot{k}_1)|\mathbf{I}) &= \mathop{\mathbb{E}}_{l\in\mathcal{K}}\left\{P_{e:1}(\dot{\mathbf{x}}_1(\dot{k}_1)|l, \mathbf{I})\right\} \\ &= \sum_{\hat{\mathbf{x}}_2(\hat{k}_2)\neq\dot{\mathbf{x}}_1(\dot{k}_1)}\sum_{q=1}^{2}\frac{\lambda_q N_0 \exp\left(-\frac{\epsilon_q}{N_0}\varphi(1)\right)}{N_0 + \epsilon_q P_t \mu_1 |\Theta(1)|^2} \\ &\qquad \times \prod_{n=2}^{N}\frac{N_0\left(1 + \exp\left(-\frac{\epsilon_q}{N_0}\varphi(n)\right)\right)}{2(N_0 + \epsilon_q P_t \mu_1 |\Theta(n)|^2)}. \end{aligned} \tag{40}$$

In a similar manner, we average $P_e(\dot{\mathbf{x}}_1(\dot{k}_1)|\mathbf{I})$ over the last condition-the residual SI term and obtain

$$\begin{aligned} &P_e(\dot{\mathbf{x}}_1(\dot{k}_1)) = \mathop{\mathbb{E}}_{\mathbf{I}}\left\{P_e(\dot{\mathbf{x}}_1(\dot{k}_1)|\mathbf{I})\right\} \\ &= P_{e:1}(\dot{\mathbf{x}}_1(\dot{k}_1)) + P_{e:2}(\dot{\mathbf{x}}_1(\dot{k}_1)) - P_{e:1}(\dot{\mathbf{x}}_1(\dot{k}_1))P_{e:2}(\dot{\mathbf{x}}_1(\dot{k}_1)), \end{aligned} \tag{41}$$

where $P_{e:1}(\dot{\mathbf{x}}_1(\dot{k}_1))$ can be derived in closed form as follows:

$$\begin{aligned} &P_{e:1}(\dot{\mathbf{x}}_1(\dot{k}_1)) = \mathop{\mathbb{E}}_{\mathbf{I}}\left\{P_{e:1}(\dot{\mathbf{x}}_1(\dot{k}_1)|\mathbf{I})\right\} \\ &= \sum_{\hat{\mathbf{x}}_2(\hat{k}_2)\neq\dot{\mathbf{x}}_1(\dot{k}_1)}\sum_{q=1}^{2}\int_0^\infty \frac{\lambda_q N_0 \exp\left(-\frac{\epsilon_q}{N_0}\varphi(1)\right)}{N_0 + \epsilon_q P_t \mu_1 |\Theta(1)|^2} f_\varphi(\varphi(1))\mathrm{d}\varphi(1) \\ &\qquad \times \prod_{n=2}^{N}\int_0^\infty \frac{N_0\left(1 + \exp\left(-\frac{\epsilon_q}{N_0}\varphi(n)\right)\right)}{2(N_0 + \epsilon_q P_t \mu_1 |\Theta(n)|^2)} f_\varphi(\varphi(n))\mathrm{d}\varphi(n) \\ &= \sum_{\hat{\mathbf{x}}_2(\hat{k}_2)\neq\dot{\mathbf{x}}_1(\dot{k}_1)}\sum_{q=1}^{2}\frac{\lambda_q N_0^2}{(N_0 + \epsilon_q P_t \mu_1 |\Theta(1)|^2)(N_0 + \epsilon_q \bar{\varphi})} \\ &\qquad \times \prod_{n=2}^{N}\frac{N_0(2N_0 + \epsilon_q \bar{\varphi})}{2(N_0 + \epsilon_q P_t \mu_1 |\Theta(n)|^2)(N_0 + \epsilon_q \bar{\varphi})}. \end{aligned} \tag{42}$$

Finally, because the incoming bit stream is equiprobable, the average BLER can be derived by averaging over the transmit OFDM block $\dot{\mathbf{x}}_1(\dot{k}_1)$ to be

$$\begin{aligned} \bar{P}_e &= \mathop{\mathbb{E}}_{\dot{\mathbf{x}}_1(\dot{k}_1)\in\mathcal{X}}\left\{P_e(\dot{\mathbf{x}}_1(\dot{k}_1))\right\} \\ &= \sum_{\dot{\mathbf{x}}_1(\dot{k}_1)\in\mathcal{X}}\Psi(\dot{\mathbf{x}}_1(\dot{k}_1))P_e(\dot{\mathbf{x}}_1(\dot{k}_1)), \end{aligned} \tag{43}$$

where

$$\Psi(\dot{\mathbf{x}}_1(\dot{k}_1)) = 1\Big/(2^{N-1}M^{T(\dot{k}_1)}) \tag{44}$$

represents the probability that the transmit OFDM block $\dot{\mathbf{x}}_1(\dot{k}_1)$ is chosen.

To the best of authors' knowledge, (43) is the most simplified and general form that we are able to obtain for the full-duplex DF relay-assisted OFDM-IM system, because the components of the summation operation in (43) only depend on the construction of the subcarrier activation patterns.

C. End-to-End Capacity Analysis

The average end-to-end capacity characterizes the transmission efficiency of the proposed OFDM-IM system assisted by full-duplex DF relaying. Again, we adopt the hop decoupling model by assuming perfect detection at the relay node[5], so that $k_1 = k_2 = k$. As a result, we can reduce (16) to be

$$\begin{aligned} &C(k|l, \mathbf{H}_1, \mathbf{H}_2, \mathbf{I}) \\ &\approx \sum_{n\in\mathcal{T}(k)}\log\left(1 + \frac{P_t}{T(k)}\min\left\{\frac{G_1(n)}{s(l,n)\varphi(n) + N_0}, \frac{G_2(n)}{N_0}\right\}\right). \end{aligned} \tag{45}$$

Let $z(n) = s(l,n)\varphi(n) + N_0$, $t_1(n) = G_1(n)/z(n)$, $t_2(n) = G_2(n)/N_0$ and $t_\Sigma(n) = \min\{t_1(n), t_2(n)\}$. Then, (45) can be rewritten as

$$C(k|\{t_\Sigma(n)|n\in\mathcal{T}(k)\}) = \sum_{n\in\mathcal{T}(k)}\log\left(1 + \frac{P_t}{T(k)}t_\Sigma(n)\right). \tag{46}$$

[5]Once more, here we adopt this assumption is only for simplifying the mathematical derivations in the following so as to achieve an insightful and closed-form approximation of the average end-to-end capacity. This is irrelevant to the actual transmission and detection procedures.

$$
\begin{aligned}
P_{e:1}(\dot{\mathbf{x}}_1(\dot{k}_1)\to\hat{\mathbf{x}}_2(\hat{k}_2)|l,\mathbf{H}_1,\mathbf{I}) &= Q\left(\sqrt{\frac{1}{N_0}\left\|\sqrt{\tfrac{P_t}{T(\dot{k}_1)}}\mathbf{H}_1\dot{\mathbf{x}}_1(\dot{k}_1)+\mathbf{S}(l)\mathbf{I}-\sqrt{\tfrac{P_t}{T(\hat{k}_2)}}\mathbf{H}_1\hat{\mathbf{x}}_2(\hat{k}_2)\right\|_F^2}\right)\\
&= Q\left(\sqrt{\frac{1}{N_0}\sum_{n=1}^{N}\left|\sqrt{P_t}h_1(n)\Theta(n)+s(l,n)I(n)\right|^2}\right)\\
&\overset{(a)}{\approx} Q\left(\sqrt{\frac{1}{N_0}\sum_{n=1}^{N}\left(\left|\sqrt{P_t}h_1(n)\Theta(n)\right|^2+|s(l,n)I(n)|^2\right)}\right)\\
&= Q\left(\sqrt{\frac{1}{N_0}\sum_{n=1}^{N}\left(P_tG_1(n)|\Theta(n)|^2+s(l,n)\varphi(n)\right)}\right)\\
&\overset{(b)}{\approx} \sum_{q=1}^{2}\lambda_q\exp\left(-\frac{\epsilon_q}{N_0}\sum_{n=1}^{N}\left(P_tG_1(n)|\Theta(n)|^2+s(l,n)\varphi(n)\right)\right)\\
&\overset{(c)}{=} \sum_{q=1}^{2}\lambda_q\prod_{n=1}^{N}\exp\left(-\frac{\epsilon_qP_t}{N_0}G_1(n)|\Theta(n)|^2\right)\exp\left(-\frac{\epsilon_q}{N_0}s(l,n)\varphi(n)\right)
\end{aligned}
\tag{32}
$$

$$
\begin{aligned}
P_{e:1}(\dot{\mathbf{x}}_1(\dot{k}_1)|l,\mathbf{I}) &= \mathop{\mathbb{E}}_{\mathbf{H}_1}\left\{P_{e:1}(\dot{\mathbf{x}}_1(\dot{k}_1)|l,\mathbf{H}_1,\mathbf{I})\right\} = \sum_{\hat{\mathbf{x}}_2(\hat{k}_2)\neq\dot{\mathbf{x}}_1(\dot{k}_1)}\mathop{\mathbb{E}}_{\mathbf{H}_1}\left\{P_{e:1}(\dot{\mathbf{x}}_1(\dot{k}_1)\to\hat{\mathbf{x}}_2(\hat{k}_2)|l,\mathbf{H}_1,\mathbf{I})\right\}\\
&= \sum_{\hat{\mathbf{x}}_2(\hat{k}_2)\neq\dot{\mathbf{x}}_1(\dot{k}_1)}\underbrace{\int_0^\infty\int_0^\infty\cdots\int_0^\infty}_{N-\text{fold}}\left(\sum_{q=1}^{2}\lambda_q\prod_{n=1}^{N}\exp\left(-\frac{\epsilon_qP_t}{N_0}G_1(n)|\Theta(n)|^2\right)\exp\left(-\frac{\epsilon_q}{N_0}s(l,n)\varphi(n)\right)\right)\prod_{n=1}^{N}f_1(G_1(n))\mathrm{d}G_1(n)\\
&= \sum_{\hat{\mathbf{x}}_2(\hat{k}_2)\neq\dot{\mathbf{x}}_1(\dot{k}_1)}\sum_{q=1}^{2}\lambda_q\prod_{n=1}^{N}\exp\left(-\frac{\epsilon_q}{N_0}s(l,n)\varphi(n)\right)\int_0^\infty\exp\left(-\frac{\epsilon_qP_t}{N_0}G_1(n)|\Theta(n)|^2\right)f_1(G_1(n))\mathrm{d}G_1(n)\\
&= \sum_{\hat{\mathbf{x}}_2(\hat{k}_2)\neq\dot{\mathbf{x}}_1(\dot{k}_1)}\sum_{q=1}^{2}\lambda_q\prod_{n=1}^{N}\frac{N_0\exp\left(-\frac{\epsilon_q}{N_0}s(l,n)\varphi(n)\right)}{N_0+\epsilon_qP_t\mu_1|\Theta(n)|^2}
\end{aligned}
\tag{37}
$$

$$
\begin{aligned}
P_{e:2}(\dot{\mathbf{x}}_1(\dot{k}_1)) &= \mathop{\mathbb{E}}_{\mathbf{H}_2}\left\{P_{e:2}(\dot{\mathbf{x}}_1(\dot{k}_1)|\mathbf{H}_2)\right\} = \sum_{\hat{\mathbf{x}}_2(\hat{k}_2)\neq\dot{\mathbf{x}}_1(\dot{k}_1)}\mathop{\mathbb{E}}_{\mathbf{H}_2}\left\{P_{e:2}(\dot{\mathbf{x}}_1(\dot{k}_1)\to\hat{\mathbf{x}}_2(\hat{k}_2)|\mathbf{H}_2)\right\}\\
&= \sum_{\hat{\mathbf{x}}_2(\hat{k}_2)\neq\dot{\mathbf{x}}_1(\dot{k}_1)}\underbrace{\int_0^\infty\int_0^\infty\cdots\int_0^\infty}_{N-\text{fold}}\left(\sum_{q=1}^{2}\lambda_q\prod_{n=1}^{N}\exp\left(-\frac{\epsilon_qP_t}{N_0}G_2(n)|\Theta(n)|^2\right)\right)\prod_{n=1}^{N}f_2(G_2(n))\mathrm{d}G_2(n)\\
&= \sum_{\hat{\mathbf{x}}_2(\hat{k}_2)\neq\dot{\mathbf{x}}_1(\dot{k}_1)}\sum_{q=1}^{2}\lambda_q\prod_{n=1}^{N}\int_0^\infty\exp\left(-\frac{\epsilon_qP_t}{N_0}G_2(n)|\Theta(n)|^2\right)f_2(G_2(n))\mathrm{d}G_2(n)\\
&= \sum_{\hat{\mathbf{x}}_2(\hat{k}_2)\neq\dot{\mathbf{x}}_1(\dot{k}_1)}\sum_{q=1}^{2}\lambda_q\prod_{n=1}^{N}\frac{N_0}{N_0+\epsilon_qP_t\mu_2|\Theta(n)|^2}
\end{aligned}
\tag{38}
$$

Hence, to derive the average end-to-end capacity, we must first obtain the distribution of $t_\Sigma(n)$. To do so, first of all, we can write the conditional PDF of $z(n)$ as

$$f_Z(z(n)|s(l,n)) = \frac{1}{s(l,n)} f_\varphi\left(\frac{z(n)-N_0}{s(l,n)}\right), \quad z(n) > N_0. \tag{47}$$

Therefore, it is easy to derive the conditional CDF of $t_1(n) = G_1(n)/z(n)$ to be

$$\begin{aligned} F_{T1}(t_1(n)|s(l,n)) &= \int_{N_0}^{\infty} F_1(z(n)t_1(n)) f_Z(z(n)|s(l,n))\mathrm{d}z(n) \\ &= 1 - \frac{\mu_1 \exp\left(-N_0 t_1(n)/\mu_1\right)}{\mu_1 + s(l,n)\bar{\varphi} t_1(n)}. \end{aligned} \tag{48}$$

Now, we can remove the condition of $F_{T1}(t_1(n)|s(l,n))$ by averaging over $s(l,n)$ and obtain

$$\begin{aligned} &F_{T1}(t_1(n)) \\ &= \begin{cases} 1 - \frac{\mu_1 \exp(-N_0 t_1(1)/\mu_1)}{\mu_1 + \bar{\varphi} t_1(1)}, & n = 1 \\ 1 - \frac{(2\mu_1 + \bar{\varphi} t_1(n)) \exp(-N_0 t_1(n)/\mu_1)}{2(\mu_1 + \bar{\varphi} t_1(n))}, & n \in \mathcal{T}(k) \backslash \{1\} \end{cases} \end{aligned} \tag{49}$$

The corresponding PDF of $t_1(n)$ can thus be deduced to be

$$\begin{aligned} &f_{T1}(t_1(n)) = \frac{\mathrm{d}F_{T1}(t_1(n))}{\mathrm{d}t_1(n)} = \\ &\begin{cases} \frac{\exp(-N_0 t_1(1)/\mu_1)[\mu_1 \bar{\varphi} + N_0(\mu_1 + \bar{\varphi} t_1(1))]}{(\mu_1 + \bar{\varphi} t_1(1))^2}, & n = 1 \\ \frac{\exp(-N_0 t_1(n)/\mu_1)[\mu_1^2 \bar{\varphi} + N_0(\mu_1 + \bar{\varphi} t_1(n))(2\mu_1 + \bar{\varphi} t_1(n))]}{2\mu_1(\mu_1 + \bar{\varphi} t_1(n))^2}, & n \in \mathcal{T}(k) \backslash \{1\} \end{cases} \end{aligned} \tag{50}$$

Likewise, we can derive the CDF and PDF of $t_2(n)$ to be

$$F_{T2}(t_2(n)) = F_2(N_0 t_2(n)) \;\Leftrightarrow\; f_{T2}(t_2(n)) = N_0 f_2(N_0 t_2(n)). \tag{51}$$

Because $t_\Sigma(n) = \min\{t_1(n), t_2(n)\}$, we can determine the CDF of $t_\Sigma(n)$ by

$$\begin{aligned} F_{T\Sigma}(t_\Sigma(n)) = F_{T1}(t_\Sigma(n)) + F_{T2}(t_\Sigma(n)) \\ - F_{T1}(t_\Sigma(n)) F_{T2}(t_\Sigma(n)). \end{aligned} \tag{52}$$

Consequently, the PDF of $t_\Sigma(n)$ can be given by

$$\begin{aligned} f_{T\Sigma}(t_\Sigma(n)) &= \frac{\mathrm{d}F_{T\Sigma}(t_\Sigma(n))}{\mathrm{d}t_\Sigma(n)} \\ &= f_{T1}(t_\Sigma(n))(1 - F_{T2}(t_\Sigma(n))) \\ &\quad + f_{T2}(t_\Sigma(n))(1 - F_{T1}(t_\Sigma(n))). \end{aligned} \tag{53}$$

Subsequently, we can apply (53) to determine the conditional end-to-end capacity on subcarrier activation pattern k by averaging $t_\Sigma(n)$, $n \in \mathcal{T}(k)$, and for a large P_t, the closed-form expression of $C(k)$ is given in (54) (shown at the top of the next page), where $\mathrm{Ei}(x) = -\int_{-x}^{\infty} \exp(-t)/t \mathrm{d}t$ denotes the exponential integral function and $\gamma \approx 0.577$ is the Euler-Mascheroni constant. Finally, we average $C(k)$ over subcarrier activation pattern k and obtain the average end-to-end capacity as follows:

$$\bar{C} = \frac{1}{2^{N-1}} \sum_{k \in \mathcal{K}} C(k). \tag{55}$$

IV. Numerical Results

To verify the analysis provided in Section III and provide comparisons between full-duplex and half-duplex relaying schemes in different aspects, we carry out related numerical simulations by Monte Carlo methods and present the generated numerical results in this section. To do so, we set up related simulation parameters as follows. To be general, we normalize the outage threshold s, noise power N_0 as well as the average channel power gain μ_1 and μ_2 in all simulations. Then, we first verify the analysis for average outage probability, BLER and end-to-end capacity with different parameters and give the simulation results in Fig. 2, Fig. 3 and Fig. 4, respectively.

First, from Fig. 2, we can see that the analytical results match the numerical results very well, which confirm the correctness of the results presented in Section III-A. Meanwhile, the effects of N and $\bar{\varphi}$ on outage performance can also be shown in this figure. As we defined in *Definition 1*, the outage event is dominated by the worse subcarrier with the smallest SINR/SNR in either the first or second hop. As a result, an increase on the number of subcarriers N will lead to worse outage performance, since the SINR/SNR of all subcarriers need to be ensured to be larger than the outage threshold s. Also, larger average power of residual SI will result in worse outage performance as well, which characterizes the SI cancellation capability of full-duplex systems. Here, we intentionally choose a small and a large $\bar{\varphi}$ (i.e. 0.1 and 10) to show the effectiveness of (28) for a wide range of $\bar{\varphi}$. Second, from Fig. 3, here we set $\bar{\varphi} = 0.1$ and we can observe that the analytical curves are accurate when the average power of residual SI is small. Increasing either the number of subcarriers N or the APM order M will lead to a higher average BLER, which is simply because it becomes more difficult to distinguish between two adjacent blocks by ML detection with PSK when either N or M goes larger. Third, from Fig. 4, as what we expect, the analytical curves approach the numerical curves when P_t becomes large, due to the approximated relation in (54). As reverse to the outage and error performance, a larger number of subcarriers N will produce a higher average end-to-end capacity, which refers to the well-known reliability-throughput trade-off in OFDM systems [46]. It is apparent that a larger average power of residual SI $\bar{\varphi}$, which indicates an inappropriately applied SI cancellation technique, will decrease the average end-to-end capacity. Again, we intentionally choose a small and a large $\bar{\varphi}$ (i.e. 0.1 and 10) to show the effectiveness of (55) for a wide range of $\bar{\varphi}$ when P_t is large.

Another interesting phenomenon that we observe from Fig. 3 is the error performance reversal for cases $\{N, M\} = \{4, 2\}$ and $\{N, M\} = \{2, 4\}$ in the low and high SNR regions. It would be difficult to rigorously explain from the analytical expression given in (43), as all these parameters are highly coupled. From a practical viewpoint, it could be explained as when the transmit power P_t is insufficient (i.e. at low SNR), whether a subcarrier is activated or not is hard to detect, since the received power on subcarriers is on a similar level to the noise power. Therefore, the index detection errors dominate compared to the symbol detection errors. On the

$$C(k) \approx \sum_{n\in\mathcal{T}(k)} \int_0^{\infty} \log\left(1+\frac{P_t}{T(k)}t_\Sigma(n)\right) f_{T\Sigma}(t_\Sigma(n))\mathrm{d}t_\Sigma(n)$$
$$= \frac{T(k)+1}{2}\exp\left(\frac{N_0(\mu_1+\mu_2)}{\mu_2\bar{\varphi}}\right)\mathrm{Ei}\left(-\frac{N_0(\mu_1+\mu_2)}{\mu_2\bar{\varphi}}\right) + T(k)\left(\log\left(\frac{P_t\mu_1\mu_2}{T(k)N_0(\mu_1+\mu_2)}\right)-\gamma\right) \quad (54)$$

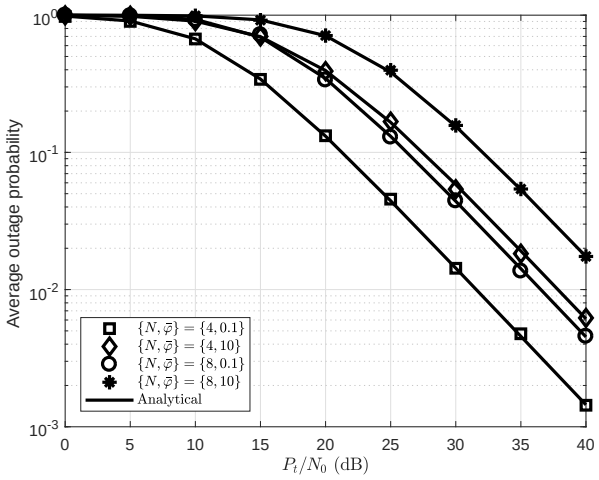

Fig. 2: Average outage probability vs. ratio of transmit power to noise power P_t/N_0 with different numbers of subcarriers N and average power of residual SI $\bar{\varphi}$.

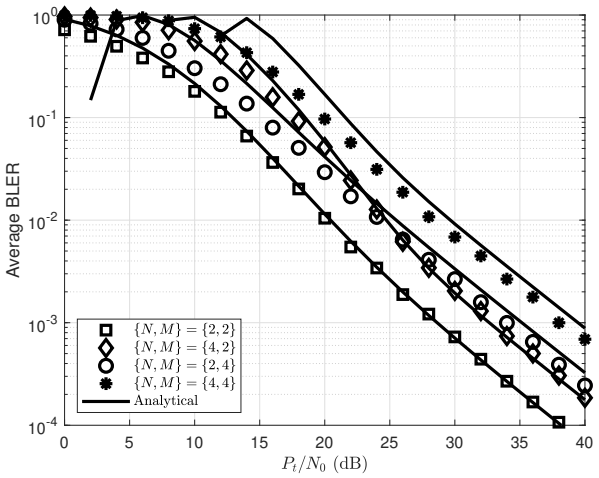

Fig. 3: Average BLER vs. ratio of transmit power to noise power P_t/N_0 with different numbers of subcarriers N and APM orders M, given $\bar{\varphi}=0.1$.

other hand, when sufficient transmit power is provided (i.e. at high SNR), it will be easier to correctly detect the indices of active subcarriers, while the symbol detection errors become the main error events.

Having substantiated the analysis in this paper, we also need to compare the performance between the proposed full-duplex system with its half-duplex counterpart in terms of outage performance, error performance and capacity, so that the superiority of the proposed system can be confirmed. To

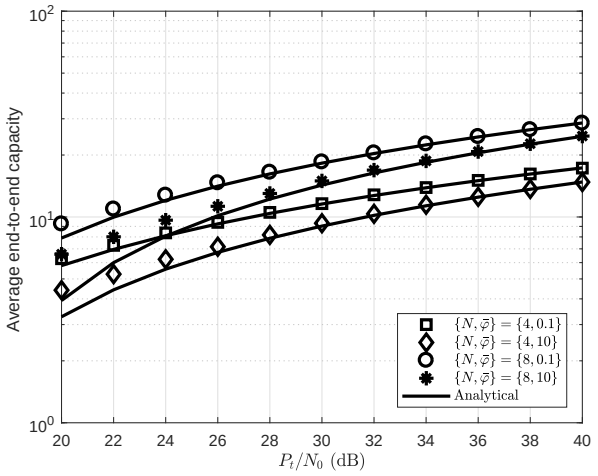

Fig. 4: Average end-to-end capacity vs. ratio of transmit power to noise power P_t/N_0 with different numbers of subcarriers N and average power of residual SI $\bar{\varphi}$.

ease the reproduction of the simulation results, we specify the configuration of the three performance metrics for half-duplex relay-assisted OFDM-IM systems as follows. First, the received OFDM block at the relay is similar to the form given in (5), but setting $\mathbf{I}=\mathbf{0}_{N\times 1}$. Therefore, when applying the half-duplex relaying protocol, the SNR of the received signal on the nth subcarrier (active) at the relay can be expressed by modifying (6) as $\mathsf{SNR}_1(k_1,l,n)=\mathsf{SINR}_1(k_1,l,n)|_{\varphi(n)=0}$. Furthermore, since the outage event is in essence defined from the perspective of end-to-end capacity, the outage threshold for half-duplex systems is $\xi=s(s+2)$ when the outage threshold is set to be s for full-duplex systems[6]. All expressions of average outage probability and BLER follow the same as given in (12), (13) and (14), (15), respectively. For the calculation of end-to-end capacity, because half-duplex relaying protocol requires two orthogonal phases for one complete transmission from source to destination via the relay, the expression of average end-to-end capacity for half-duplex relaying should thereby be modified as $\bar{C}_{half}=\frac{1}{2}\bar{C}|_{\varphi(n)=0,n\in\mathcal{N}}$. We carry out the simulations of the proposed full-duplex relay-assisted OFDM-IM system in terms of three performance evaluation metrics with regard to the average power of residual SI $\bar{\varphi}$ and adopt the half-duplex relay-assisted OFDM-IM system as the comparison benchmark. Numerical results are shown in Fig. 5. From this figure, we can see that there exists a critical average power of residual SI $\bar{\varphi}_c$, below which the full-duplex relaying is preferable in terms of outage performance and end-

[6]More details and explanations of this modification can be found in [24], [25].

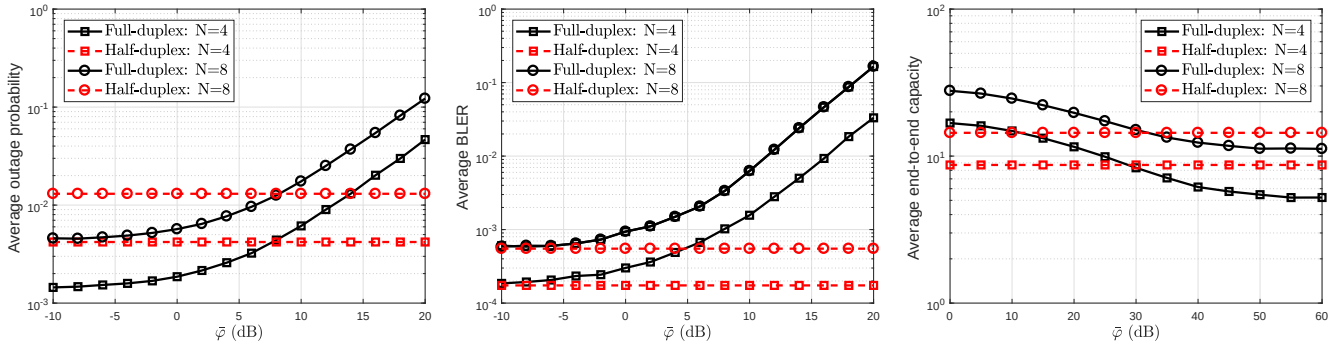

(a) (b) (c)

Fig. 5: Comparisons between full-duplex and half-duplex relay-assisted OFDM-IM systems given $P_t = 40$ dB and $M = 2$: (a) average outage probability; (b) average BLER; (c) average end-to-end capacity.

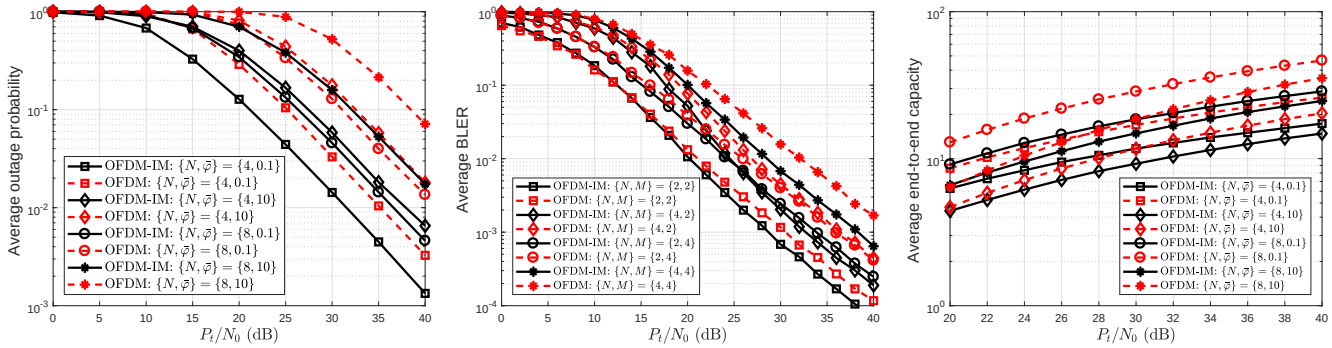

(a) (b) (c)

Fig. 6: Comparisons between full-duplex relay-assisted OFDM-IM and OFDM systems: (a) average outage probability; (b) average BLER (given $\bar{\varphi} = 0.1$); (c) average end-to-end capacity.

to-end capacity. Also, the number of subcarriers will have only a trivial impact on this critical average power. On the other hand, the introduction of full-duplex relaying will have an inevitable and negative influence on the error performance, as the residual SI term is additive according to (5). Therefore, in order to possess the benefits of full-duplex relaying, we need to apply appropriate SI cancellation techniques and ensure a small average power of residual SI.

Furthermore, to confirm the superiority of full-duplex relay-assisted OFDM-IM compared to full-duplex relay-assisted OFDM without IM, we also carry out corresponding simulations in terms of the three performance evaluation metrics with regard to the ratio of transmit power to noise power P_t/N_0. The numerical results are presented in Fig. 6. From this figure, it is shown that our proposed scheme outperforms the full-duplex relay-assisted OFDM scheme without IM in terms of outage and error performance. On the other hand, the conventional OFDM scheme achieves a higher end-to-end capacity. These results indicate that the proposed scheme is more suited for reliability-critical networks, e.g. Internet of Things, alerting networks, wireless sensor networks etc. [47]–[49], instead of throughput-critical networks, e.g. networks of stream media, virtual reality and Big Data etc. [50]–[53].

V. Conclusion

In this paper, we proposed a full-duplex relay-assisted OFDM-IM system, in which the transmitted signal from the source will be decoded and forwarded to the destination by a full-duplex DF relay. By adopting the full-duplex relaying protocol, we might be able to achieve better outage performance and a higher end-to-end capacity in comparison with half-duplex relaying, as long as the average power of residual SI can be reduced to a certain level by applying proper SI cancellation techniques. Also, we analyzed the proposed full-duplex relay-assisted OFDM-IM system in terms of average outage probability, BLER and end-to-end capacity, and derived or approximated these performance evaluation metrics in closed form. All these analyses have been verified by numerical results generated by Monte Carlo simulations. Meanwhile, we carried out relevant simulations to compare the performance between half-duplex and full-duplex relaying schemes and confirm the performance superiority of the proposed full-duplex relay-assisted OFDM-IM system.

Overall, by the analytical and numerical results provided in this paper, a comprehensive framework for analyzing full-duplex relay-assisted OFDM-IM can be constructed, which would be easily modified to analyze other extended cases with more complicated channel models and relaying protocols. Some future research directions that are worth in-

vestigating include but are not limited to: 1) combinations between full-duplex relay-assisted OFDM-IM and other advanced subcarrier activation schemes, e.g. multi-mode OFDM-IM, enhanced OFDM-IM and generalized OFDM-IM etc.; 2) employing different full-duplex forwarding protocols apart from DF relaying, e.g. various amplify-and-forward (AF) relaying, compress-and-forward (CF) relaying and adaptive relaying etc.; 3) Applying the proposed full-duplex relay-assisted OFDM-IM system in multi-relay and/or multi-user scenarios; 4) Considering an adaptive power allocation scheme over active subcarriers instead of the simple but inefficient uniform power allocation scheme.

ACKNOWLEDGMENT

The authors would like to thank the anonymous reviewers for their constructive comments which help improve the quality of this manuscript.

REFERENCES

[1] E. Dahlman, S. Parkvall, and J. Skold, *4G: LTE/LTE-Advanced for Mobile Broadband*. Elsevier Science, 2013.

[2] S. Gokceli, E. Basar, M. Wen, and G. K. Kurt, "Practical implementation of index modulation-based waveforms," *IEEE Access*, vol. 5, pp. 25 463–25 473, Nov. 2017.

[3] B. Farhang-Boroujeny and H. Moradi, "OFDM inspired waveforms for 5G," *IEEE Communications Surveys Tutorials*, vol. 18, no. 4, pp. 2474–2492, Fourthquarter 2016.

[4] E. Basar, "Index modulation techniques for 5G wireless networks," *IEEE Communications Magazine*, vol. 54, no. 7, pp. 168–175, Jul. 2016.

[5] R. Fan, Y. J. Yu, and Y. L. Guan, "Generalization of orthogonal frequency division multiplexing with index modulation," *IEEE Transactions on Wireless Communications*, vol. 14, no. 10, pp. 5350–5359, Oct. 2015.

[6] N. Ishikawa, S. Sugiura, and L. Hanzo, "Subcarrier-index modulation aided OFDM - will it work?" *IEEE Access*, vol. 4, pp. 2580–2593, May 2016.

[7] M. Wen, E. Basar, Q. Li, B. Zheng, and M. Zhang, "Multiple-mode orthogonal frequency division multiplexing with index modulation," *IEEE Transactions on Communications*, vol. 65, no. 9, pp. 3892–3906, Sept. 2017.

[8] X. Cheng, M. Zhang, M. Wen, and L. Yang, "Index modulation for 5G: striving to do more with less," *IEEE Wireless Communications*, vol. 25, no. 2, pp. 126–132, Apr. 2018.

[9] J. Mrkic, E. Kocan, and M. Pejanovic-Djurisic, "Index modulation techniques in OFDM relay systems for 5G wireless networks," in *Proc. IEEE TSP*, Barcelona, Spain, Jul. 2017.

[10] Q. Ma, P. Yang, L. Dan, X. He, Y. Xiao, and S. Li, "OFDM-IM-aided cooperative relaying protocol for cognitive radio networks," in *Proc. IEEE SPAWC*, Sapporo, Japan, July 2017.

[11] S. Dang, J. P. Coon, and G. Chen, "Adaptive OFDM with index modulation for two-hop relay-assisted networks," *IEEE Transactions on Wireless Communications*, vol. 17, no. 3, pp. 1923–1936, Mar. 2018.

[12] S. Dang, G. Chen, and J. P. Coon, "Power allocation for adaptive OFDM index modulation in cooperative networks," in *Proc. IEEE GLOBECOM*, Singapore, Dec. 2017.

[13] Z. Wang, S. Dang, and D. T. Kennedy, "Multi-hop index modulation-aided OFDM with decode-and-forward relaying," *IEEE Access*, pp. 1–1, 2018.

[14] S. Dang, G. Chen, and J. P. Coon, "Outage performance of two-hop OFDM with index modulation and multi-carrier relay selections," *IEEE Wireless Communications Letters*, 2018.

[15] J. Crawford and Y. Ko, "Cooperative OFDM-IM relay networks with partial relay selection under imperfect CSI," *IEEE Transactions on Vehicular Technology*, pp. 1–1, 2018.

[16] S. H. Song, A. F. Almutairi, and K. B. Letaief, "Outage-capacity based adaptive relaying in LTE-advanced networks," *IEEE Transactions on Wireless Communications*, vol. 12, no. 9, pp. 4778–4787, Sept. 2013.

[17] G. Liu, F. R. Yu, H. Ji, V. C. M. Leung, and X. Li, "In-band full-duplex relaying: a survey, research issues and challenges," *IEEE Communications Surveys Tutorials*, vol. 17, no. 2, pp. 500–524, Secondquarter 2015.

[18] Z. Zhang, X. Chai, K. Long, A. V. Vasilakos, and L. Hanzo, "Full duplex techniques for 5G networks: self-interference cancellation, protocol design, and relay selection," *IEEE Communications Magazine*, vol. 53, no. 5, pp. 128–137, May 2015.

[19] Z. Zhang, K. Long, A. V. Vasilakos, and L. Hanzo, "Full-duplex wireless communications: Challenges, solutions, and future research directions," *Proceedings of the IEEE*, vol. 104, no. 7, pp. 1369–1409, Jul. 2016.

[20] B. Debaillie, D. J. van den Broek, C. Lavín, B. van Liempd, E. A. M. Klumperink, C. Palacios, J. Craninckx, B. Nauta, and A. Pärssinen, "Analog/RF solutions enabling compact full-duplex radios," *IEEE Journal on Selected Areas in Communications*, vol. 32, no. 9, pp. 1662–1673, Sept. 2014.

[21] M. Chung, M. S. Sim, J. Kim, D. K. Kim, and C. b. Chae, "Prototyping real-time full duplex radios," *IEEE Communications Magazine*, vol. 53, no. 9, pp. 56–63, Sept. 2015.

[22] G. Chen, Y. Gong, P. Xiao, and J. A. Chambers, "Physical layer network security in the full-duplex relay system," *IEEE Transactions on Information Forensics and Security*, vol. 10, no. 3, pp. 574–583, Mar. 2015.

[23] M. Mohammadi, H. A. Suraweera, Y. Cao, I. Krikidis, and C. Tellambura, "Full-duplex radio for uplink/downlink wireless access with spatially random nodes," *IEEE Transactions on Communications*, vol. 63, no. 12, pp. 5250–5266, Dec. 2015.

[24] S. Dang, G. Chen, and J. P. Coon, "Outage performance analysis of full-duplex relay-assisted device-to-device systems in uplink cellular networks," *IEEE Transactions on Vehicular Technology*, vol. 66, no. 5, pp. 4506–4510, May 2017.

[25] ——, "Multicarrier relay selection for full-duplex relay-assisted OFDM D2D systems," *IEEE Transactions on Vehicular Technology*, pp. 1–1, 2018.

[26] M. Mokhtar, N. Al-Dhahir, and R. Hamila, "OFDM full-duplex DF relaying under I/Q imbalance and loopback self-interference," *IEEE Transactions on Vehicular Technology*, vol. 65, no. 8, pp. 6737–6741, Aug. 2016.

[27] S. Rajkumar and J. S. Thiruvengadam, "Outage analysis of OFDM based cognitive radio network with full duplex relay selection," *IET Signal Processing*, vol. 10, no. 8, pp. 865–872, Oct. 2016.

[28] S. Dang, J. P. Coon, and G. Chen, "Resource allocation for full-duplex relay-assisted device-to-device multicarrier systems," *IEEE Wireless Communications Letters*, vol. 6, no. 2, pp. 166–169, Apr 2017.

[29] J. Proakis and M. Salehi, *Digital Communications*, ser. McGraw-Hill International Edition. McGraw-Hill, 2008.

[30] Q. Huang, M. Ghogho, J. Wei, and P. Ciblat, "Practical timing and frequency synchronization for OFDM-based cooperative systems," *IEEE Transactions on Signal Processing*, vol. 58, no. 7, pp. 3706–3716, July 2010.

[31] P. Yang, M. D. Renzo, Y. Xiao, S. Li, and L. Hanzo, "Design guidelines for spatial modulation," *IEEE Communications Surveys Tutorials*, vol. 17, no. 1, pp. 6–26, Firstquarter 2015.

[32] M. D. Renzo and H. Haas, "Bit error probability of SM-MIMO over generalized fading channels," *IEEE Transactions on Vehicular Technology*, vol. 61, no. 3, pp. 1124–1144, Mar. 2012.

[33] M. Wen, X. Cheng, M. Ma, B. Jiao, and H. V. Poor, "On the achievable rate of OFDM with index modulation," *IEEE Transactions on Signal Processing*, vol. 64, no. 8, pp. 1919–1932, Apr. 2016.

[34] S. Dang, J. P. Coon, and G. Chen, "Outage performance of two-hop OFDM systems with spatially random decode-and-forward relays," *IEEE Access*, vol. 5, pp. 27 514–27 524, Nov. 2017.

[35] X. Wu, Y. Shen, and Y. Tang, "Propagation characteristics of the full-duplex self-interference channel for the indoor environment at 2.6 GHz," in *Proc. IEEE APSURSI*, Jul. 2014.

[36] M. Duarte, C. Dick, and A. Sabharwal, "Experiment-driven characterization of full-duplex wireless systems," *IEEE Transactions on Wireless Communications*, vol. 11, no. 12, pp. 4296–4307, Dec. 2012.

[37] D. Zhao, H. Zhao, M. Jia, and W. Xiang, "Smart relaying for selection combining based decode-and-forward cooperative networks," *IEEE Communications Letters*, vol. 18, no. 1, pp. 74–77, Jan. 2014.

[38] E. Basar, "On multiple-input multiple-output OFDM with index modulation for next generation wireless networks," *IEEE Transactions on Signal Processing*, vol. 64, no. 15, pp. 3868–3878, Aug. 2016.

[39] A. Ghasemi and E. S. Sousa, "Fundamental limits of spectrum-sharing in fading environments," *IEEE Transactions on Wireless Communications*, vol. 6, no. 2, pp. 649–658, Feb. 2007.

[40] K. Hamdi, W. Zhang, and K. B. Letaief, "Power control in cognitive radio systems based on spectrum sensing side information," in *Proc. IEEE ICC*, Glasgow, UK, June 2007, pp. 5161–5165.

[41] W. Yang and Y. Cai, "On the performance of the block-based selective OFDM decode-and-forward relaying scheme for 4G mobile communication systems," *Journal of Communications and Networks*, vol. 13, no. 1, pp. 56–62, Feb. 2011.

[42] P. Raviteja, Y. Hong, and E. Viterbo, "Spatial modulation in full-duplex relaying," *IEEE Communications Letters*, vol. 20, no. 10, pp. 2111–2114, Oct. 2016.

[43] W. Wang and R. Wu, "Capacity maximization for OFDM two-hop relay system with separate power constraints," *IEEE Transactions on Vehicular Technology*, vol. 58, no. 9, pp. 4943–4954, Nov. 2009.

[44] D. S. Michalopoulos, J. Schlenker, J. Cheng, and R. Schober, "Error rate analysis of full-duplex relaying," in *Proc. IEEE WDD*, Niagara Falls, ON, Canada, Aug. 2010.

[45] E. Basar, U. Aygolu, E. Panayırci, and H. V. Poor, "Orthogonal frequency division multiplexing with index modulation," *IEEE Transactions on Signal Processing*, vol. 61, no. 22, pp. 5536–5549, Nov. 2013.

[46] S. Sadr, A. Anpalagan, and K. Raahemifar, "Radio resource allocation algorithms for the downlink of multiuser OFDM communication systems," *IEEE Communications Surveys Tutorials*, vol. 11, no. 3, pp. 92–106, Aug. 2009.

[47] G. Chen, J. Tang, and J. P. Coon, "Optimal routing for multihop social-based D2D communications in the Internet of Things," *IEEE Internet of Things Journal*, vol. 5, no. 3, pp. 1880–1889, June 2018.

[48] Z. Wang, L. Zhang, A. S. Edmonds, and S. Dang, "Network-based anti-theft alert system using dynamic hybrid TOA/AOA algorithm," *Journal of Communications*, vol. 11, no. 8, 2016.

[49] F. Li and Z. Lv, "Reliable vehicle type recognition based on information fusion in multiple sensor networks," *Computer Networks*, vol. 117, pp. 76–84, 2017.

[50] Z. Lv, T. Yin, Y. Han, Y. Chen, and G. Chen, "WebVR-web virtual reality engine based on P2P network," *Journal of Networks*, vol. 6, no. 7, p. 990, 2011.

[51] J. Yang, S. He, Y. Lin, and Z. Lv, "Multimedia cloud transmission and storage system based on internet of things," *Multimedia Tools and Applications*, vol. 76, no. 17, pp. 17 735–17 750, 2017.

[52] Z. Lv, H. Song, P. Basanta-Val, A. Steed, and M. Jo, "Next-generation big data analytics: State of the art, challenges, and future research topics," *IEEE Transactions on Industrial Informatics*, vol. 13, no. 4, pp. 1891–1899, Aug. 2017.

[53] H. Fu, Z. Li, Z. Liu, and Z. Wang, "Research on big data digging of hot topics about recycled water use on micro-blog based on particle swarm optimization," *Sustainability*, vol. 10, no. 7, pp. 1–15, 2018.

Jinxian Zhao Jinxian Zhao graduated from Harbin Engineering University with the majors of Communication Engineering and Control Theory & Control Engineering, respectively. He is currently a professor with the School of Electronics and Information Engineering, Heilongjiang University of Science and Technology, and dedicates to the signal and information processing. He has tens of papers published in international journals and conference proceedings. Meanwhile, he also participated in a series of research projects sponsored by National Natural Science Foundation of China and three research projects sponsored by the local municipal government in Heilongjiang.

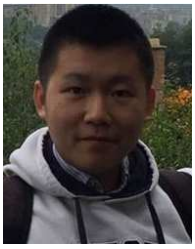

Shuping Dang (S'13, M'18) received the B.Eng (Hons) degree in Electrical and Electronic Engineering from the University of Manchester (with first class honors) and the B.Eng in Electrical Engineering and Automation from Beijing Jiaotong University in 2014 via a joint '2+2' dual-degree program. He also received the D.Phil in Engineering Science from University of Oxford in 2018. He was also a *Certified LabVIEW Associate Developer* (CLAD) by National Instrument (NI) (2014 - 2016). Dr. Dang joined in the R&D center, Huanan Communication Co., Ltd. as a Technical Director (TD) after graduating from University of Oxford and is currently working as a Postdoctoral Fellow with the Computer, Electrical and Mathematical Science and Engineering Division, King Abdullah University of Science and Technology (KAUST). He serves as a reviewer for IEEE TRANSACTIONS ON WIRELESS COMMUNICATIONS, IEEE TRANSACTIONS ON COMMUNICATIONS, IEEE TRANSACTIONS ON VEHICULAR TECHNOLOGY, IEEE SYSTEMS JOURNAL, IEEE ACCESS, DIGITAL SIGNAL PROCESSING (Springer), EURASIP JOURNAL ON WIRELESS COMMUNICATIONS AND NETWORKING (Springer) as well as the TPC member of a number of leading conferences in communication engineering, including IEEE ICC, Globecom and VTC etc. His current research interests include artificial intelligence assisted communications, novel modulation schemes, cooperative communications, wireless signal processing and 5G communication system design.

Zhongli Wang graduated from University of Science and Technology Beijing with his majors of Communication Engineering and Control Theory & Control Engineering, respectively. He is currently an associate professor with the College of Electrical and Information Engineering, Beihua University and dedicates to the investigations of wireless communications, signal processing, pattern recognition and embedded systems. He has tens of papers published in international journals and proceedings and wrote three textbooks. He also participated in two research projects sponsored by National Natural Science Foundation of China, four research projects sponsored by the local municipal government and three research projects sponsored by Beihua University.